Wide Cross-species RNA-Seq Comparison Reveals Convergent Molecular Mechanisms Involved in Nickel Hyperaccumulation Across Dicotyledons

Vanesa Sanchez Garcia de La Torre, Clarisse Majorel-Loulergue, Guillem J. Rigaill, Dubiel A. Gonzalez, Ludivine Soubigou-Taconnat, Yohan Pillon, Louise Barreau, Sébastien Thomine, Bruno Fogliani, Valérie Burtet-Sarramegna, et al.

New Phytologist

Wide Cross-species RNA-Seq Comparison Reveals Convergent Molecular Mechanisms Involved in Nickel Hyperaccumulation Across Dicotyledons

Journal:	*New Phytologist*
Manuscript ID	NPH-MS-2020-32526.R1
Manuscript Type:	MS - Regular Manuscript
Date Submitted by the Author:	n/a
Complete List of Authors:	García de la Torre, Vanesa; I2BC, Cell Biology Majorel, Clarisse; Univesity of New Caledonia, ISEA Rigaill, Guillem; IPS2, PMIN; Université d'Evry Val d'Essonne, Laboratoire de Mathématiques at Modélisation d'Evry (LaMME) González, Dubiel; Universidad Agraria de La Habana (UNAH), Department of Biology Soubigou-Taconnat, Ludivine; Institute of Plant Sciences Paris-Saclay (IPS2), 91192 Pillon, Yohan; Institut de recherche pour le developpement, LSTM Barreau, Louise; I2BC, Cell Biology Thomine, Sébastien; CNRS, Institute for Integrative Biology of the Cell (I2BC) 1 Fogliani, Bruno; Institut Agronomique néo-Calédonien (IAC), Equipe ARBOREAL; Univesity of New Caledonia, ISEA Burtet-Sarramegna, Valerie; Univesity of New Caledonia, ISEA Merlot, Sylvain; CNRS, I2BC
Key Words:	Hyperaccumulator, Metal, Nickel, RNA-Seq, IREG/Ferroportin, Convergence, Noccaea caerulescens

Wide Cross-species RNA-Seq Comparison Reveals Convergent Molecular Mechanisms Involved in Nickel Hyperaccumulation Across Dicotyledons

Vanesa S. Garcia de la Torre[1§], Clarisse Majorel-Loulergue[2], Guillem J. Rigaill[3,4,5], Dubiel A. Gonzalez[6], Ludivine Soubigou-Taconnat[3,5], Yohan Pillon[7], Louise Barreau[1], Sébastien Thomine[1], Bruno Fogliani[2,8], Valérie Burtet-Sarramegna[2], Sylvain Merlot[1*]

[1]*Université Paris-Saclay, CEA, CNRS, Institute for Integrative Biology of the Cell (I2BC), 91198, Gif-sur-Yvette, France.*

[2]*Institute of Exact and Applied Sciences (ISEA), Université de la Nouvelle-Calédonie, BP R4, 98851, Nouméa cedex, New Caledonia*

[3]*Université Paris-Saclay, CNRS, INRAE, Univ Evry, Institute of Plant Sciences Paris-Saclay (IPS2), 91405, Orsay, France.*

[4]*Laboratoire de Mathématiques et Modélisation d'Evry (LaMME), Université d'Evry, CNRS, ENSIIE, USC INRAE, 23 bvd de France, 91037, Evry cedex, France*

[5]*Université de Paris, CNRS, INRAE, Institute of Plant Sciences Paris-Saclay (IPS2), 91405, Orsay, France*

[6]*Universidad Agraria de La Habana (UNAH), Departamento de Biologia, 32700, Mayabeque, Cuba*

[7]*Laboratoire des Symbioses Tropicales et Méditerranéennes (LSTM), IRD, INRAE, CIRAD, Montpellier SupAgro, Univ. Montpellier, 34398, Montpellier cedex, France*

[8]*Institut Agronomique néo-Calédonien (IAC), Equipe ARBOREAL, BP 73, 98890, Païta, New Caledonia*

[§]Present address: Molecular Genetics and Physiology of Plants (MGPP), Faculty of Biology and Biotechnology, Ruhr University Bochum, 44801 Bochum, Germany

*Corresponding author: sylvain.merlot@i2bc.paris-saclay.fr ; Phone: +33-169824642

Total word count (w/o summary): 5903

Summary: 198

Introduction: 802

Materials and Methods: 1822

Results: 1913

Discussion: 1366

Number of Figures: 5

Fig. 1, Fig. 2, Fig.5 should be published in color

Number of tables: 1

Supporting Information: Fig: 7; Notes: 1, Tables: 6.

Keywords: Hyperaccumulator, Metal, Nickel, RNA-Seq, IREG/Ferroportin, Convergence, *Noccaea caerulescens*.

Summary

- The Anthropocene epoch is associated with the spreading of metals in the environment increasing oxidative and genotoxic stress on organisms. Interestingly, about 500 plant species growing on metalliferous soils acquired the capacity to accumulate and tolerate tremendous amount of nickel in their shoots. The wide phylogenetic distribution of these species suggests that nickel hyperaccumulation evolved multiple times independently. However, the exact nature of these mechanisms and whether they have been recruited convergently in distant species is not known.
- To address these questions, we have developed a cross-species RNA-Seq approach combining differential gene expression analysis and cluster of orthologous group annotation to identify genes linked to nickel hyperaccumulation in distant plant families.
- Our analysis reveals candidate orthologous genes encoding convergent function involved in nickel hyperaccumulation, including the biosynthesis of specialized metabolites and cell wall organization. Our data also point out that the high expression of IREG/Ferroportin transporters recurrently emerged as a mechanism involved in nickel hyperaccumulation in plants. We further provide genetic evidence in the hyperaccumulator *Noccaea caerulescens* for the role of the NcIREG2 transporter in nickel sequestration in vacuoles.
- Our results provide molecular tools to better understand the mechanisms of nickel hyperaccumulation and study their evolution in plants.

Introduction

Because of their chemical and biochemical properties, transition metals play fundamental roles in living organisms. However, when present in excess in the environment they induce adverse effects on biological systems producing oxidative and genotoxic stresses or causing secondary deficiency of essential elements because of competition (Waldron *et al.*, 2009; Andresen *et al.*, 2018). Even though they contain metal levels toxic to most plant species, metalliferous soils of geogenic or anthropogenic origin are colonized by specific floras adapted to these high concentrations of metals. While the majority of metallophyte species exclude metals from their tissues, over 700 species have acquired the capacity to accumulate and tolerate tremendous amount of metals in their shoot (van der Ent *et al.*, 2013; Reeves *et al.*, 2018). Plants hyperaccumulating nickel (>1000 mg/kg shoot dry weight) represent, with around 520 species, the vast majority of metal hyperaccumulators (Reeves *et al.*, 2018), likely because of the frequent occurrence of outcrops originating from ultramafic rocks, including serpentine soils, in regions of high biodiversity such as Cuba, New Caledonia or the Mediterranean basin. The large phylogenetic distribution of nickel hyperaccumulators in various plant families further suggest that nickel hyperaccumulation appeared independently several times during plant evolution (Kramer, 2010; Cappa & Pilon-Smits, 2014). However, whether the mechanisms allowing hyperaccumulation have been recruited convergently or are specific to different plant families is still poorly known.

As for other metals, the hyperaccumulation of nickel requires very efficient uptake by the roots, translocation of nickel to the shoot and its accumulation in leaf cells. The hyperaccumulation of nickel in leaves requires strong detoxification mechanisms involving antioxydant and metal-chelating molecules, as well as the sequestration of nickel in specific compartments (Verbruggen *et al.*, 2009; Kramer, 2010; Clemens, 2019). In most of the cases, nickel is stored in the vacuoles of epidermal cells away from photosynthetic tissues (Küpper et al., 2001; Broadhurst et al., 2004; Bidwell et al., 2004; Mesjasz-Przybylowicz et al., 2016; van der Ent et al., 2019), but nickel enrichment was also observed in the apoplast and cell walls surrounding epidermal cells (Krämer *et al.*, 2000; Bidwell *et al.*, 2004; van der Ent *et al.*, 2019).

In the field of metal hyperaccumulation, most of the molecular studies have been focused on the deciphering of zinc and cadmium accumulation in Brassicaceae species related to *A. thaliana*. Genetic and transcriptomic studies performed on *Arabidopsis halleri* and *Noccaea caerulescens* indicated that metal hyperaccumulation is associated with high and constitutive expression of genes encoding metal transporters, enzymes involved in the biosynthesis of metal chelators and proteins involved in oxidative stress responses

(Becher *et al.*, 2004; Dräger *et al.*, 2004; Weber *et al.*, 2004; Hammond *et al.*, 2006; Shahzad *et al.*, 2010). In *A. halleri,* it was further shown that knocking down the expression of the highly expressed *HEAVY METAL ATPASE 4* transporter gene reduces zinc accumulation, thus demonstrating the essential role of *HMA4* in zinc hyperaccumulation (Hanikenne *et al.*, 2008). These data indicated that metal hyperaccumulation essentially evolved from a dysregulation of genes involved in basic mechanisms of metal homeostasis.

Despite the essential role of nickel in plants to sustain the activity of urease, our knowledge of the molecular mechanisms involved in nickel homeostasis is still scarce. In *Arabidopsis thaliana,* members of the IRT/ZIP and IREG/Ferroportin transporter families have been shown to play a role in nickel uptake and distribution (Schaaf *et al.*, 2006; Morrissey *et al.*, 2009; Nishida *et al.*, 2011). Furthermore, genes encoding IREG/Ferroportin transporters have been shown to be expressed at higher levels in nickel hyperaccumulators compared to related non-accumulators from the Brassicaceae, Rubiaceae and Asteraceae families (Halimaa *et al.*, 2014; Merlot *et al.*, 2014; Meier *et al.*, 2018). A recent transcriptomic study performed in roots of the non-accumulator *A. thaliana* revealed that high nickel treatment induces the downregulation of genes associated with cell walls, suggesting that the response to high nickel targets cell wall functions (Lešková *et al.*, 2019). In addition, several organic molecules, including histidine, nicotianamine and organic acids, have been shown to form complexes with nickel and have been proposed to play a role in hyperaccumulation (Krämer *et al.*, 1996; Vacchina *et al.*, 2003; Callahan *et al.*, 2012). However, whether these elements participate in the complex nickel hyperaccumulation trait still needs to be supported by functional and genetic evidences.

Here, we have developed an RNA-Seq approach combining differential gene expression analysis and cluster of orthologous group (COG) annotation to identify orthologous genes that have been convergently selected in plants to support nickel hyperaccumulation. Our cross-species comparative analysis performed on leaf transcriptomes of a wide diversity of dicotyledon families reveals several COGs associated with nickel hyperaccumulation including genes involved in metal transport, the biosynthesis of specialized metabolites and cell wall organization. We further provide genetic evidence in the nickel hyperaccumulator *Noccaea caerulescens* that the IREG/Ferroportin transporter NcIREG2 is involved in nickel sequestration into vacuoles.

Material and Methods

Plant material and sample collection

Leaves of nickel hyperaccumulator plants belonging to 5 distinct plant families (Jestrow *et al.*, 2012; Jaffré *et al.*, 2013; Borhidi *et al.*, 2016; Gonneau *et al.*, 2014), Brassicaceae [*Noccaea caerulescens subsp. firmiensis* (*Ncfi*)], Cunoniaceae [*Geissois pruinosa (Gpru)*], Euphorbiaceae [*Leucocroton havanensis (Lhav)*], Rubiaceae [*P. costivenia (Pcos)*, *P. gabriellae (Pgab)*, *Psychotria grandis (Pgra)*], Salicaceae [*Homalium kanaliense (Hkan)*], and leaves of related non-nickel hyperaccumulators, Brassicaceae [*N. caerulescens* 'Viviez' (*Ncviv*), *N. montana* (*Nmon*)], Cunoniaceae [*G. racemosa (Grac)*], Euphorbiaceae [*Lasiocroton microphyllus (Lmic)*], Rubiaceae [*P. revoluta* (*Prev*), *P. semperflorens (Psem)*], Salicaceae [*H. betulifolium (Hbet)*], were collected on individual plants growing in their natural environment and localized by GPS (Supporting Information Table S1). We complied with local regulation for the access to these genetic resources. For each sample, a fraction of leaves was washed with water and dried for elemental analysis, and the other fraction fixed on site with liquid N_2 (*Gpru*, *Grac*, *Pgab*, *Psem*) or with RNA*later* (Sigma Aldrich) and stored at 4°C (*Ncfi, Ncviv, Nmon, Lhav, Lmic, Pcos, Pgra, Prev, Hkan, Hbet*). RNA*later* was removed in the laboratory and leaves were immediately stored at -80°C before RNA extraction.

Additionally, to generate reference transcriptomes, *Ncfi* and *Nmon* were grown in hydroponic condition in a climatic chamber (9 h light, 150 $\mu E.m^{-2}.s^{-1}$, 21 ºC/17 ºC day/night, 70 % humidity) for 7 weeks using a modified Hoagland's solution (Lanquar *et al.*, 2010), containing 20 µM Fe-HBED (Van Iperen International) and 37.5 µM $NiCl_2$. *L. havanensis* seeds were cultured *in vitro* on Murashige & Skoog Agar medium supplemented with 3.2 mM $NiSO_4$, as described (Gonzalez & Matrella, 2013).

A specimen of *Cunonia capensis* (*Ccap*) was obtained from a specialized plant nursery (Ets. Railhet, France) and grown in a green-house on coconut coir supplemented with fertilizer.

Phylogenetic analysis

Phylogenetic trees of nickel hyperaccumulator and non-accumulator species were constructed with FigTree using the checklist of metal hyperaccumulators from (Reeves *et al.*, 2018), the APG III classification (Chase & Reveal, 2009) and the plant time-calibrated tree from (Magallón *et al.*, 2015). Phylogenetic analysis of IREG/FPN protein family was performed with CLC Genomics Workbench v20 software (Qiagen).

RNA sequencing

Total RNA from leaves was extracted with RNeasy Plant Mini kit (Qiagen) for *Noccaea* species, Qiagen hybrid method for woody plants for *Psychotria* species from Cuba

(Johnson *et al.*, 2012), CTAB-PVP method for *Geissois* and *Psychotria* species from New Caledonia (Johnson *et al.*, 2012), and TRI Reagent (Sigma-Aldrich) for *Leucocroton*, *Lasiocroton* and *Homalium* species. DNA was removed from all RNA samples by RNeasy Plant Mini kit on-column DNase I treatment.

RNA quality control, preparation of cDNA libraries, sequencing and raw reads processing were performed by the POPS transcriptomic platform (IPS2, Orsay, France). Libraries were prepared from 1 µg of total RNA using TruSeq Stranded mRNA kit (Illumina) and sequenced with an Illumina HiSeq2000 sequencing system in 100bp paired-end mode. Libraries meant to be directly compared were multiplexed and sequenced in a single run. Adaptors and low-quality pair-end sequences were removed from the raw reads and the ribosomal RNA was filtered using the SortMeRNA algorithm (Kopylova *et al.*, 2012). We obtained between 27 and 106 million reads per libraries (Supporting Information Table S2).

De novo transcriptome assembly and annotation

The transcriptome sequences of *Ncfi*, *Nmon*, *Pgab*, *Psem*, *Pgra*, *Pcos*, *Prev*, *Gpru*, *Grac*, *Hkan*, *Hbet*, *Lhav* and *Lmic* were obtained independently by *de novo* assembly of paired-end reads using CLC Genomics Workbench v9 software (Qiagen). A single library per species was used to minimize genetic variability. Assembly parameters were set as default, except similarity (0.95), length fraction (0.75) and the word size was optimized for each sample (Supporting Information Table S2). The quality of *de novo* assemblies was assessed by Transrate v1.0.3 using trimmed read sequences (Smith-Unna et al., 2016) and BUSCO v4.0.4 using Viridiplantae odb10 lineage dataset (Simão *et al.*, 2015). The sequences of the resulting contigs were blasted (Blastx, E-value of ≤ 10E-6) against the Viridiplantae protein database (NCBI) and putative function annotated by Gene Ontology (cut-off = 55; GO weight = -5) using Blast2GO (Conesa *et al.*, 2005). Filtered contigs for length (≥ 200 nt) and expression (TPKM > 1) were translated for the longest Open Reading Frame. Translated sequences longer than 20 amino acids, together with *Arabidopsis thaliana* protein sequences (TAIR10, www.arabidopsis.org) were analyzed by OrthoFinder to annotate Clusters of Orthologous Group (COG) (Emms & Kelly, 2015).

Differential gene expression analysis

For each pair of species, read count estimation was carried out using CLC Genomics Workbench v9 software by mapping sequencing reads of each sample replicate (default parameters, except similarity: 0.875 and length fraction: 0.75) to the transcriptome of the nickel hyperaccumulator species used as the reference. Statistical analyses to identify Differentially Expressed Genes (DEGs) were performed using the edgeR Bioconductor

package (Robinson *et al.*, 2010). To examine transcript abundance, reads per kilobase million (RPKM) were calculated. To evaluate the influence of the reference transcriptome, we additionally performed swapping analyses using the transcriptome of the non-accumulator species as reference (Supporting Information Table S2). The association of contigs between transcriptomes of a pair of species was established by reciprocal Blast.

Multiple-testing analysis

Following differential gene expression analyses, we recovered 25,313 COGs containing at least one DEG and collected for each of these COG a number of test statistics (i.e. p-value of all the contigs of this COG) per plant family. We further discarded COGs for which we had test statistics for less than 3 plant families (15,052 COGs), and finally kept 10,261 COGs to perform the multiple-testing analysis using the Cherry R package version 0.6-12 (Goeman *et al.*, 2018). We first provided the complete list of the corresponding 121,133 p-values to Cherry and used the Simes inequality with the hommelFast function in R. Then for every COG and plant family, we identified contigs significantly up-regulated (FC>2) and down-regulated and used Cherry to get a lower bound on the number of H1 contigs (with a simultaneous 95% confidence using the pickSimes function in R). For every COG, we counted the number of plant families with at least one up-regulated contig (respectively down-regulated) identified by Cherry. Finally, COGs containing up-regulated or down-regulated contigs in hyperaccumulators species in at least 3 different plant families were selected as candidates COGs associated with nickel hyperaccumulation.

Molecular cloning

Predicted full-length coding region of *NcfilREG2*, *GpruIREG1* and *LhavIREG2* were amplified from leaf cDNAs of the corresponding species, using high-fidelity Phusion polymerase (Thermo Scientific) with gene specific primers containing AttB recombination sequences (Supporting Information Table S6). PCR products were first recombined into pDONOR207 (Invitrogen) and then in pDR195-GTW or pMDC83 for expression in yeast and *N. caerulescens* respectively (Curtis & Grossniklaus, 2003; Oomen *et al.*, 2008). Artificial miRNA construct targeting *NcfilREG2* was designed using the WMD3-Web microRNA Designer (http://wmd3.weigelworld.org). The amiRNA was engineered as previously described (Schwab *et al.*, 2006), by PCR using the pRS300 backbone and specific primers (Supporting Information Table S6). The *NcfilREG2*-amiRNA precursor was recombined in pDONOR207 and then into the vector pK7GW2D (Karimi *et al.*, 2002). All constructs were confirmed by restriction analysis and sequencing.

Functional analyses of IREG/Ferroportin in Saccharomyces cerevisiae

IREG/Ferroportin coding regions cloned into pDR195-GTW, as well as pDR195-AtIREG2 (Schaaf *et al.*, 2006), were transformed by the lithium acetate/PEG method into the *Saccharomyces cerevisiae* BY4741 strain complemented by a functional *HIS3* gene. Yeast sensitivity to nickel was scored by drop assay using serial dilution on histidine-free YNB agar medium containing 20 mM MES (pH5.5), supplemented or not with $NiCl_2$. Empty pDR195 vector was used as control. Experiments were repeated twice with three independent transformants.

Functional analysis of NcfiIREG2 in transgenic plants

pK7GW2D-*NcfiIREG2-amiRNA* and *pMDC83-NcfiIREG2* were transformed into *N. caerulescens* subsp. *firmiensis* by *Rhizobium rhizogenes* (Arqua1 strain) mediated *in vitro* root transformation (Lin *et al.*, 2016). Transformed roots were selected using GFP fluorescence under a Leica MZ FLIII Fluorescence Stereo Microscope. Non-transformed roots were cut once a week until the whole root system was transgenic.

Independent lines transformed with pK7GW2D-*NcfiIREG2-amiRNA* were then transferred in hydroponic culture as described above for a week and then with the nutrient solution supplemented with 37.5 µM $NiCl_2$ for 4 weeks. For each transgenic line, the root system was divided in two samples for RT-qPCR and elemental analysis.

Elemental analysis

Dried environmental leaf samples were mineralized by HNO_3. Multi-elemental analyses were performed using ICP-AES (LAMA laboratory, IRD, New Caledonia) or MP-AES.

Plant samples from hydroponic cultures were washed twice with ice-cold 10 mM Na_2EDTA and twice with ice-cold ultrapure water. Samples were dried at 65 ºC for 16 hours, weighed and then digested with 70 % HNO_3 and H_2O_2 for a total of 8 h with temperature ramping from 80 to 120 °C. Elemental analyses were performed using MP-AES (Agilent 4200, Agilent Technologies) and metal concentration was calculated by comparison with a metal standard solution.

Confocal Imaging

Roots transformed with pMDC83-*NcfiIREG2* were stained with 10 µg/ml propidium iodide (PI) and imaged on a Leica SP8X inverted confocal microscope (IMAGERIE-Gif platform) with laser excitation at 488 nm and collection of emitted light at 495–550 nm for GFP and 600–650 nm for PI.

Quantitative RT-PCR analyses

Total RNA from *Noccaea* species was extracted with RNeasy Plant Mini kit or with TRI Reagent for *Ncfi* transgenic roots. Total RNA from leaves of *Gpru* and *Ccap* was extracted with the CTAB-PVP method as described above. DNA was removed from all

RNA samples by RNeasy Plant Mini kit on-column DNase I treatment. RNA (1 µg) were converted to cDNA by random priming using SuperScript III or IV First-Strand reverse transcriptase (Invitrogen) according to the manufacturer's instructions. Quantitative PCR analysis were performed on a LightCycler 96 using LightCycler 480 SYBR Green I Master Mix (Roche) with the following conditions: Initial denaturation (95 ºC, 300 s), followed by 40 cycles of amplification (95 °C, 15 s; 60 °C, 15 s; 72 °C, 15 s), and a melting curve (95 °C, 10 s; 65 ºC, 30 s and 95 ºC, 1s). Sequence information for Ccap (sample TIUZ) was obtained from the 1KP project (Matasci *et al.*, 2014). Reference genes for *Noccaea species* (*6-phosphogluconate dehydrogenase decarboxylating 3, Nc6PGDH*, Ncfi_contig_3009), and *Cunoniaceae* species (*Histone deacetylase 15*, *GpruHDAC15*, Gpru_contig_14406) were selected from our RNA-Seq analyses. Specific primers for *IREG/Ferroportin* and reference genes were designed to produce amplicons of 100-200 nt (Supporting Information Table S6). Relative gene expression was calculated using the primer efficiency correction method (Pfaffl, 2001). Two technical replicates were used for each sample.

General statistics

Sample exploration and replication of sequencing data analysis were conducted using limma R package (Ritchie *et al.*, 2015), correlation analyses were conducted by linear regression using generic stats functions of R software and Heat-map clustering was carried out using heatmap.2 function of the gplots R package (R Development Core Team, 2015).

Data availability

Raw sequence files, read count files and *de novo* assembled transcriptomes are publicly available in the NCBI's Gene Expression Omnibus under the SuperSeries accession number GSE116054 or SubSeries accession numbers GSE115411 (Brassicaceae), GSE116051 (Rubiaceae, New Caledonia), GSE116050 (Rubiaceae, Cuba), GSE116048 (Cunoniaceae), GSE116052 (Salicaceae) and GSE116049 (Euphorbiaceae).

Results

Sampling nickel hyperaccumulators from a wide diversity of plant families

Nickel hyperaccumulators are found as herbaceous plants, shrubs or trees scattered in 50 plants families almost exclusively in eudicots (45 families), in both Rosids and Asterids clades (Fig. **1**). Some families such as Brassicaceae (87 taxons), Asteraceae (45 taxons) and families of the COM clade comprising Cunoniaceae (48 taxons), Euphorbiaceae (42 taxons) and Salicaceae (38 taxons) are enriched in nickel hyperaccumulators (Jaffré *et al.*, 2013; Reeves *et al.*, 2018). The distribution of nickel hyperaccumulators suggests that this complex trait appeared independently several times during plant evolution but also that some families may have a predisposition to develop this trait.

To cover this large diversity, we sampled leaves of 7 nickel hyperaccumulators from 5 genera (i.e, *Noccaea, Psychotria*, *Geissois*, *Homalium*, *Leucocroton*) corresponding to Brassicaceae, Rubiaceae and the families of the COM clade Cunoniaceae, Salicaceae and Euphorbiaceae. These samples have been collected in their natural environment on ultramafic soils in France, New Caledonia and Cuba and the elemental analysis of these samples confirmed the nickel hyperaccumulator status of the corresponding species. For each hyperaccumulator, we also collected leaves of a closely related species or accession not hyperaccumulating nickel (Table **1**; Supporting Information Fig. S1, Table S1). Both nickel hyperaccumulators and the corresponding non-hyperaccumulator species were collected in the same geographic area, and when it was possible non-hyperaccumulator species were collected on ultramafic soils (i.e. *N. montana, P. semperflorens* and *H. betulifolium*).

Identification of genes differentially expressed between hyperaccumulators and related non-accumulators

To identify genes differentially expressed between nickel hyperaccumulator and closely related non-accumulator species, we performed RNA sequencing (RNA-Seq) using Illumina paired-end technology (Supporting Information Fig. S2). In absence of genomic reference sequences for these species, we assembled *de novo* the sequence of expressed genes for 13 selected species using short paired-end Illumina reads. These newly generated transcriptomes contain between 41,843 and 87,243 contigs for a total assembly size ranging from 35 Mbp to 49 Mbp and a N50 ranging from 692 to 1735 bp (Table **1**, Supporting Information Table S2). With the exception of *N. montana*, these *de novo* assemblies received a TransRate score ranging from 0.31 to 0.49 and the analysis with BUSCO indicates that they contain from 61% to 89% of complete genes with 3% to

9% of missing genes (Supporting Information Table S2). These parameters indicate that the quality of these *de novo* assemblies is in the range of the assemblies usually obtained for plant transcriptomes with this sequencing technology. The significant higher number of contigs and the lower scores obtained for *Noccaea montana* is likely the result of the allogamous reproduction of *N. montana* increasing genetic diversity and thus affecting *de novo* assembly. Subsequent annotation of these transcriptomes using Blastx interrogation of Viridiplantae proteins database revealed significant homologies for 56 % of the contigs on average (E-value ≤10E−6). These annotated reference transcriptomes constitute a unique and comprehensive resource for molecular studies on plant groups of high interest.

The reads from each environmental sample replicates were then mapped to the nickel hyperaccumulator reference transcriptome to identify differentially expressed (DE) genes in 8 pairs of species (or accessions), each containing a hyperaccumulator and a related non-accumulator. The fraction of DE genes ranged from 2 % to 29 % (Fold Change ≥ 2, *FDR* ≤ 0.05), depending on the pair of species considered (Fig. **2a**; Supporting Information Fig. S3, Table S4). To evaluate the influence of the choice of the reference transcriptome, we performed swapping analysis. To perform this analysis, we calculated the read count for each contig using the transcriptome of the non-accumulator species as reference and we performed the same transcriptomic comparison as before. We then compared the fold change of the contigs obtained with the hyperaccumulator and the non-accumulator transcriptomes successively used as references (Supporting Information Fig. S4). This analysis revealed that the results were strongly correlated in most pair of species (r = 0.81-0.85; P-value < 0.05). The lower correlation (r = 0.70) obtained when using the non-accumulator *N. montana* transcriptome as reference is likely the result of the lower quality of the transcriptome assembly for this species. Overall, the results indicated that the choice of the reference transcriptome when studying closely related species had only a marginal influence on the identification of DE genes.

Identification of biological functions associated with nickel hyperaccumulation in distant families

To determine if dysregulated molecular and metabolic pathways are shared by nickel hyperaccumulators from distant plant families, it was necessary to compare their transcriptomes altogether with a functional emphasis. To this aim, we classified the gene products into Clusters of Orthologous Groups (COG). Combining the 13 reference transcriptomes, 443,400 contigs (66.5% of total) were assigned to 46,458 COGs

(Supporting Information Table S3), and 25,313 COGs included at least one DE gene in one plant family. Following the differential gene expression analysis in the different plant families, we performed a multiple-testing analysis at the COGs level using the R Cherry package (Goeman & Solari, 2011). We selected up-regulated and down-regulated COGs containing genes more expressed, and less expressed respectively, in hyperaccumulators from at least 3 different plant families. This analysis revealed 26 groups, including 15 up-regulated COGs and 11 down-regulated COGs (Fig. **2b**; Supporting Information Table S5). The functional annotation of these COGs indicated that the most represented categories in up-regulated COGs (Fig. **2b, c**) correspond to class I transposable elements (TEs), known as retrotransposons and to genes involved in the biosynthesis and metabolism of specialized metabolites. In addition to organic acids and nitrogen/oxygen ligands (e.g. histidine and nicotianamine acid) that are known nickel ligands, more recent studies have highlighted the role of the phenylpropanoid compounds coumarins and flavonoids as potential metal ligands involved in metal transport, tolerance and accumulation in plants (Kasprzak *et al.*, 2015; Tsai & Schmidt, 2017; Corso *et al.*, 2018). Therefore, the high expression of genes coding for enzymes involved in the biosynthesis of specific metabolites such as UDP-glucose:anthocyanidin/flavonol 3-O-glucosyltransferase (COG 35) or BAHD acyltransferase (COG 44) could therefore lead to an increased synthesis of metal ligands in nickel hyperaccumulators.

On the other hand, the most represented categories in down-regulated COGs correspond to genes involved in response to stress and in cell wall biogenesis or organization (Fig. **2d**). This latter category includes COGs corresponding to expansin (COG 75), xyloglucan endotransglucosylase/hydrolase (COG 109) and pectin acetylesterase (COG 423). Because of their capacity to bind positively charged metals, cell walls may regulate the apoplastic mobility of metals or be a reservoir for metals in nickel hyperaccumulators (Krämer *et al.*, 2000; Krzesłowska, 2011; Le Gall *et al.*, 2015). However, it is difficult to predict the consequences of a reduced expression of these genes on cell wall properties regarding metals binding in nickel hyperaccumulators.

The high expression of IREG/Ferroportin transporters in leaves has a conserved function in nickel hyperaccumulation

Our analysis points to IREG/Ferroportin transporters (COG 1981) as some of the most robustly up-regulated function associated with nickel hyperaccumulation in several plant families (Fig. **2c**; Supporting Information Table S5). Phylogenetic analysis revealed that Brassicaceae species, including *N. caerulescens*, contain 2 gene clusters, represented

by *A. thaliana* IREG1 and IREG2, belonging to COG 1981 (Supporting Information Fig. S5). These transporters were shown to localize on different membranes and therefore proposed to play distinct functions in metal transport (Schaaf *et al.*, 2006; Morrissey *et al.*, 2009). In several species from the Euphorbiaceae, Salicaceae, Cunoniaceae and Rubiaceae families, we also observe a duplication of IREG/Ferroportin genes. However, these transporters do not cluster with AthaIREG1 or AthaIREG2 and it is therefore not possible to infer their specific function. Genes encoding IREG/Ferroportin transporters are significantly more expressed (from 4 to 800-fold increase) in several nickel hyperaccumulator species from the Brassicaceae, Rubiaceae and Euphorbiaceae families compared to their related non-accumulator species. Very recently, the high expression in leaves of an IREG/Ferroportin gene from the Asteraceae species *Senecio coronatus* was associated with the capacity to hyperaccumulate nickel (Meier *et al.*, 2018). Together, these results strongly support the hypothesis that the high expression of *IREG/Ferroportin* in leaves may play an essential and conserved role in nickel hyperaccumulation in a wide diversity of plant families in both Asterid and Rosid clades.

In the selected pairs of species of the Salicaceae and Cunoniaceae families originating from New Caledonia, we did not detect differential expression of *IREG/Ferroportin* genes (Fig. **2c**). However, the analysis of our RNA-Seq data indicates that *IREG/Ferroportin* genes are highly expressed in both hyperaccumulator and non-accumulator species from these families compared to non-accumulators from Brassicaceae and Euphorbiaceae families (Supporting Information Fig. **S6a**). Furthermore, the unique *IREG/Ferroportin* gene (COG 1981) detected in the hyperaccumulator *Geissois pruinosa* is 60-times more expressed than its orthologue in the non-accumulator Cunoniaceae species *Cunonia capensis* from South Africa (Supporting Information Fig. **S6b**). The high expression of *IREG*/*Ferroportin* genes in non-accumulator species endemic to New Caledonia might be a genetic footprint of nickel tolerance and hyperaccumulation caused by the recent (<35 Ma) colonization of this island then probably fully covered by an ultramafic rock layer rich in nickel (Pillon *et al.*, 2010, 2014). After adaptive radiation, some species that have colonized more recently exposed non-ultramafic areas might have lost some of the important functions necessary for the full expression of the nickel tolerance and hyperaccumulation traits while still expressing IREG/Ferroportin at high levels.

IREG/Ferroportin transporters have a conserved function in vacuolar sequestration of nickel in hyperaccumulators

To provide functional evidence for the conserved role of plant IREG/Ferroportin in nickel hyperaccumulation, we expressed in yeast IREG/Ferroportin orthologs cloned from 3 nickel hyperaccumulators from the distant families Brassicaceae, Cunoniaceae and Euphorbiaceae (Fig. **3**). The expression of these transporters increases yeast resistance to nickel. These results are consistent with a conserved function of plant IREG/Ferroportin as metal exporters, driving nickel out of the cytosol in the extracellular medium or in intracellular stores and thus reducing cytosolic toxicity.

We then wanted to investigate the biological function of IREG/Ferroportin in nickel hyperaccumulation *in planta* using *Noccaea caerulescens* as a model. We chose to target *NcIREG2,* the ortholog of *Arabidopsis thaliana IREG2*, because it shows the strongest expression in both shoot and roots of the nickel hyperaccumulator *N. caerulescens subsp. firmiensis* when compared with the non-accumulator *Noccaea caerulescens 'Viviez'* (Fig. **4**; Supporting Information Table S4). We first used *Rhizobium rhizogenes* root transformation to express a C-terminal GFP tagged version of NcfiIREG2 in *N. caerulescens* subsp. *firmiensis*. NcfiIREG2-GFP is able to complement the nickel hypersensitive phenotype of the *A. thaliana ireg2* mutant indicating that this fusion protein is functional (Supporting Information Fig. **S7**). Confocal imaging of *N. caerulescens* transgenic roots shows that NcfiIREG2-GFP localizes on the membrane of the vacuole suggesting a role of this transporter in nickel storage in this intracellular compartment (Fig. **5a**). To support this hypothesis, we used the same transformation strategy to silence the expression of *NcfiIREG2* using artificial amiRNA technology. We generated 8 independent composite transgenic lines displaying different degrees of *NcfiIREG2* silencing (Fig. **5b**). Elemental analysis of these transgenic lines revealed a decrease of nickel concentration in roots that strongly correlates (R^2 = 0.97, P-value < 0.001) with *NcfiIREG2* expression (Fig. **5c**). In contrast, the concentration of nickel in the shoots of these lines does not correlate with *NcfiIREG2* expression in roots (R^2 = 0.45). Together, these results provide evidences that NcfiIREG2 contributes to the accumulation of nickel in the roots of *Noccaea caerulescens* subsp. *firmiensis* by driving nickel sequestration in vacuoles. However, the expression of *NcIREG2* in roots does not seem to be a limiting factor for the transport of nickel to the shoot in *N. caerulescens* subsp. *firmiensis*.

Discussion

The development of RNA-Seq technologies has opened the possibility to study non-model species at the molecular level. Yet, comparative biology has not fully benefited from this revolution because of the difficulty to quantitatively compare transcriptomes from distant species (Roux *et al.*, 2015). In this study, we have used a combination of cross-species comparative transcriptomics analysis, COG annotation and multiple-testing analysis to identify genes associated with nickel hyperaccumulation in a wide diversity of plant families. While pairwise comparisons between a nickel hyperaccumulator and a related non-hyperaccumulator species identified a high number of candidate DE genes, it is expected that a large proportion of these candidate DE genes are not directly linked to the nickel hyperaccumulation trait but also to other traits differentiating these species. On the other hand, pairwise comparison of closely related species or accessions with a distinctive hyperaccumulation phenotype may also fail to reveal mechanisms involved in this multigenic trait as for example observed for IREG/ Ferroportin genes in *Geissois* species from New Caledonia (Fig. **2c**, Fig. **S6**). Thus, we focused our analyses on the identification of convergent mechanisms between families (Fig. **2a**; Supporting Information Fig. **S3**). This strategy allowed the identification of a limited number of candidate DE genes playing a conserved function in nickel hyperaccumulation. This strategy may fail to identify molecular mechanisms specific to a group of plants (e.g. family, genus). However, a similar approach could likely be used to identify such specific mechanisms but would require to increase the number of species within this group.

The high expression of IREG/Ferroportin transporters was previously linked to nickel hyperaccumulation in Brassicaceae and Asteraceae species (Halimaa *et al.*, 2014; Meier *et al.*, 2018). Our results support these findings and further indicates that IREG/Ferroportin transporters have been recurrently recruited as a convergent mechanism for nickel hyperaccumulation in a wide diversity of plant species. It is also interesting to notice that we did not identify other families of metals transporters suggesting that, besides IREG/Ferroportin, diverse metal transporter families may have been recruited to support other important steps of nickel accumulation in leaves of distant hyperaccumulator species. Importantly, this result *a posteriori* validates our cross-species comparative approach to identify genes playing a convergent role in nickel hyperaccumulation.

Our results also point to a convergent role for several functions involved in the biogenesis and organization of cell walls and in the synthesis of specialized metabolites (Fig. **2c,d**).

The high expression of several genes involved in the metabolism of phenylpropanoid compounds is linked to the hyperaccumulation trait in several families. Coumarins and flavonoids have the capacity to bind metals and have been previously linked to iron nutrition and cadmium accumulation (Kasprzak *et al.*, 2015; Tsai & Schmidt, 2017; Corso *et al.*, 2018). These results suggest that nickel hyperaccumulators synthesize specialized metabolites involved in the detoxification and transport of nickel. However, the functional annotation of the selected COGs does not allow to pinpoint specific pathways. Comparative metabolomic analyses of nickel hyperaccumulator and related non-accumulator species may identify specialized metabolites associated with nickel hyperaccumulation and therefore establish a direct link between identified COGs and specialized metabolites biosynthetic pathways. A recent report showed that the excess of nickel in *A. thaliana* leads to a reduced expression of genes associated with cell walls of root cells (Lešková *et al.*, 2019). Accordingly, we observed a lower expression of COGs associated with cell wall in several hyperaccumulator species. Interestingly, our analysis also revealed the up-regulation of COG 19, corresponding to the cell wall-associated kinase family (WAKL) in nickel hyperaccumulators (Fig. **2c**). The expression of members of the WAKL family has been shown to be induced by metals in plants and the increased expression of *WAKL4* in *A. thaliana* increases tolerance to nickel (Hou *et al.*, 2005). Together, these results suggest that a modification of the cell wall structure, at least in specific tissues, could play a conserved role in nickel tolerance and hyperaccumulation in plants.

We also identified several COGs corresponding to Class I retrotransposon up-regulated in nickel hyperaccumulating species. The expression of these elements is known to be responsive to stress conditions and their transposition can generate several types of mutations that can result in the inactivation of gene function or in increased gene expression by cis-addition (Casacuberta & González, 2013; Makarevitch *et al.*, 2015). In the metal hyperaccumulator species *A. halleri*, Class I retrotransposons are linked to the triplication of the *HMA4* gene and may account for the high expression of this metal transporter essential for zinc hyperaccumulation (Hanikenne *et al.*, 2008). It is therefore tempting to speculate that transposable elements are involved in the evolution of the nickel hyperaccumulation trait by altering the activity of some important genes.

Although metal hyperaccumulators are not easily amenable to genetic engineering, molecular genetic studies are necessary to demonstrate the role of candidate genes in this complex trait (Hanikenne *et al.*, 2008). To support the essential role of IREG/Ferroportin in nickel accumulation, we performed molecular and genetic studies in roots of the hyperaccumulator *N. caerulescens subsp. firmiensis* (Fig. **5**). These results

558 demonstrated that NcfiIREG2 localizes on the vacuole and that decreasing *NcfiIREG2*
559 expression in roots strongly affects nickel accumulation (Fig. **5b**). These results provide
560 a genetic evidence supporting a role of *NcIREG2* in the storage of nickel in the vacuoles
561 of *N. caerulescens* cells. Surprisingly, the silencing of *NcIREG2* in roots did not lead to
562 a significant increase in nickel accumulation in leaves (Fig. **5c**). This result might appear
563 as counterintuitive because the sequestration of metals in root cells has been proposed
564 to be a factor limiting their translocation and therefore their accumulation in the shoot of
565 hyperaccumulators. Our results rather suggest that the expression of *NcIREG2* in roots
566 of *N. caerulescens subsp. firmiensis* is not a factor limiting the hyperaccumulation of
567 nickel in leaves. This conclusion is further supported by the parallel comparison of
568 *NcIREG2* expression and nickel accumulation in *N. caerulescens subsp. firmiensis* and
569 *N. caerulescens* 'Viviez'. This analysis indicates that there is no negative correlation
570 between the expression of *NcIREG2* in roots and the capacity to accumulate nickel in
571 shoots (Fig. **4**). This conclusion does not rule out that the expression of *NcIREG2* in roots
572 may limit the translocation of nickel to shoots in other *Noccaea* accessions or species
573 such as *N. montana* (Fig. **4**) or *N. japonica* as very recently proposed (Nishida *et al.*,
574 2020). In contrast, the high expression of *NcIREG2* and the consecutive sequestration
575 of nickel in shoots might create a sink effect favoring the transfer of nickel from roots to
576 shoots in *N. caerulescens subsp. firmiensis*. To directly demonstrate the major role of
577 *NcIREG2* in nickel hyperaccumulation, it will be necessary to further develop
578 transformation protocols of *N. caerulescens* to modify the expression of this gene in
579 shoots.
580 Based on our wide cross-species transcriptomic analysis and functional evidences
581 obtained in transgenic *N. caerulescens*, we propose that IREG/Ferroportin transporters
582 play a conserved and essential role in the storage of nickel in the vacuole of leaf cells in
583 a wide range of nickel hyperaccumulating species. This role was previously proposed for
584 the transporter PgIREG1 from the nickel hyperaccumulator *P. gabriellae* (Merlot *et al.*,
585 2014). However, we cannot completely exclude that some IREG/Ferroportin orthologues
586 differentially expressed in hyperaccumulators might localize on the plasma membrane
587 to transport nickel out of cells as this was proposed for the *A. thaliana* IREG1 transporter
588 (Morrissey *et al.*, 2009). In the context of nickel hyperaccumulation, these transporters
589 might facilitate cell-to-cell transport of nickel or transport nickel out of epidermal cells
590 leading to its accumulation in the cell walls (Krämer et al., 2000; van der Ent et al., 2019).
591 In the context of sustainable development, nickel hyperaccumulators are now viewed as
592 crops to extract and recycle metals from large areas of metalliferous soils (Grison, 2015;
593 Nkrumah *et al.*, 2016). As for other crops, we foresee that the molecular knowledge
594 obtained in our study could become instrumental for marker-assisted selection of

595 cultivars or molecular monitoring of agricultural practices to improve nickel
596 phytoextraction. This work provides a framework to identify additional key genes from
597 root transcriptomes involved in the efficient uptake and translocation of nickel to the
598 leaves. The identification of all molecular steps from uptake in roots to sequestration in
599 leaves is necessary to fully understand this complex trait.

Acknowledgments

We thank professor Rosalina Berazaín Iturralde (JBN, Cuba) for invaluable information on the Cuban flora, Louis-Charles Brinon (IAC, New Caledonia) for sample collection in New Caledonia, Christelle Espagne for technical assistance, Véronique Brunaud and Marie-Laure Martin-Magniette (IPS2, France) for guidance on *de novo* assembly and biostatistical analysis, and Mark G. M. Aarts (WUR, Netherlands) for the *Noccaea* root transformation protocol.

This work was supported by Grants ANR-13-ADAP-0004 (SM, BF, VBS) and CNRS Defi Enviromics Gene-4-Chem to SM, a SCAC fellowship from the French Embassy in Cuba to DAG and SM and an ATIGE grant from Genopole to GJR. This work has benefited from the core facilities of Imagerie-Gif, a member of Infrastructures en Biologie Santé et Agronomie (IBiSA), supported by France BioImaging Grant ANR-10INBS-04-01 and the Saclay Plant Science Labex Grant ANR-11-IDEX-0003-0. The POPS platform benefits from the support of the LabEx Saclay Plant Sciences-SPS (ANR-10-LABX-0040-SPS). We thank the South Province of New Caledonia and the Prefecture of Aveyron for plant collection authorizations.

Author contributions

BF, VBS and SM designed the project; VSG, CML, DAG, BF, VBS and SM collected plant samples; VSG, CML, DAG, LB performed experiments; LST supervised RNA-Seq sequencing; VSG, GJR, YP, ST and SM analyzed the data; VSG, ST and SM wrote the manuscript; all authors commented and approved the content of the manuscript.

References

Andresen E, Peiter E, Kupper H. **2018**. Trace metal metabolism in plants. *Journal of Experimental Botany* **69**: 909–954.

Becher M, Talke IN, Krall L, Krämer U. **2004**. Cross-species microarray transcript profiling reveals high constitutive expression of metal homeostasis genes in shoots of the zinc hyperaccumulator *Arabidopsis halleri*. *Plant Journal* **37**: 251–268.

Bidwell SD,Crawford SA, Woodrow IE, Sommer-Knudsen J, Marshall AT. **2004**. Sub-cellular localization of Ni in the hyperaccumulator, *Hybanthus floribundus* (Lindley) F. Muell. *Plant, Cell & Environment* **27**: 705–716.

Borhidi AL, Oviedo-Prieto R, Fernández-Zequeira M. **2016**. Nuevos resultados de la revisión taxonómica de los géneros *Palicourea* y *Psychotria* (Rubiaceae, Psuchotrieae) en Cuba. *Acta Botanica Hungarica* **58**: 1–48.

Broadhurst CL, Chaney RL, Angle JS, Erbe EF, Maugel TK. **2004**. Nickel localization and response to increasing Ni soil levels in leaves of the Ni hyperaccumulator *Alyssum murale*. *Plant and Soil* **265**: 225–242.

Callahan DL, Roessner U, Dumontet V, De Livera AM, Doronila A, Baker AJ, Kolev SD. **2012**. Elemental and metabolite profiling of nickel hyperaccumulators from New Caledonia. *Phytochemistry* **81**: 80–89.

Cappa JJ, Pilon-Smits EA. **2014**. Evolutionary aspects of elemental hyperaccumulation. *Planta* **239**: 267–275.

Casacuberta E, González J. **2013**. The impact of transposable elements in environmental adaptation. *Molecular Ecology* **22**: 1503–1517.

Chase MW, Reveal JL. **2009**. A phylogenetic classification of the land plants to accompany APG III. *Botanical Journal of the Linnean Society* **161**: 122-127.

Clemens S. **2019**. Metal ligands in micronutrient acquisition and homeostasis. *Plant, Cell & Environment* **42**: 2902-2912.

Conesa A, Götz S, García-Gómez JM, Terol J, Talón M, Robles M. **2005**. Blast2GO: A universal tool for annotation, visualization and analysis in functional genomics research. *Bioinformatics* **21**: 3674–3676.

Corso M, Schvartzman MS, Guzzo F, Souard F, Malkowski E, Hanikenne M, Verbruggen N. **2018**. Contrasting cadmium resistance strategies in two metallicolous populations of *Arabidopsis halleri*. *New Phytologist* **218**: 283–297.

Curtis MD, Grossniklaus U. **2003**. A Gateway Cloning Vector Set for High-Throughput Functional Analysis of Genes in Planta **133** : 462–469.

Dräger DB, Desbrosses-Fonrouge AG, Krach C, Chardonnens AN, Meyer RC, Saumitou-Laprade P, Krämer U. **2004**. Two genes encoding *Arabidopsis halleri* MTP1

metal transport proteins co-segregate with zinc tolerance and account for high MTP1 transcript levels. *Plant J* **39**: 425–439.

Emms DM, Kelly S. **2015**. OrthoFinder: solving fundamental biases in whole genome comparisons dramatically improves orthogroup inference accuracy. *Genome Biology* **16**: 1–14.

van der Ent A, Baker AJM, Reeves RD, Pollard AJ, Schat H. **2013**. Hyperaccumulators of metal and metalloid trace elements: Facts and fiction. *Plant and Soil* **362**: 319–334.

van der Ent A, Spiers KM, Brueckner D, Echevarria G, Aarts MGM, Montargès-Pelletier E. 2019. Spatially-resolved localization and chemical speciation of nickel and zinc in *Noccaea tymphaea* and *Bornmuellera emarginata*. *Metallomics* **11**: 2052–2065.

Le Gall H, Philippe F, Domon J-M, Gillet F, Pelloux J, Rayon C. **2015**. Cell Wall Metabolism in Response to Abiotic Stress. *Plants* **4**: 112–166.

Goeman JJ, Solari A. **2011**. Multiple Testing for Exploratory Research. *Statistical Science* **26**: 584–597.

Goeman JJ, Solari A, Meijer RJ. **2019**. Cherry: Multiple testing methods for exploratory research *R package version 0.6-13*.

Gonneau C, Genevois N, Frerot H, Sirguey C, Sterckeman T. **2014**. Variation of trace metal accumulation, major nutrient uptake and growth parameters and their correlations in 22 populations of *Noccaea caerulescens*. *Plant and Soil* **384**: 271–287.

Gonzalez DA, Matrella S. **2013**. Nickel hyperaccumulation 'in vitro' by *Leucocroton havanensis* (Euphorbiaceae). *Revista del Jardín Botánico Nacional* **34**–**35**: 83–88.

Grison C. **2015**. Combining phytoextraction and ecocatalysis: a novel concept for greener chemistry, an opportunity for remediation. *Environmental Science and Pollution Research* **22**: 5589–5591.

Halimaa P, Lin YF, Ahonen VH, Blande D, Clemens S, Gyenesei A, Haikio E, Karenlampi SO, Laiho A, Aarts MG, *et al.* 2014. Gene expression differences between *Noccaea caerulescens* ecotypes help to identify candidate genes for metal phytoremediation. *Environmental Science & Technology* **48**: 3344–3353.

Hammond JP, Bowen H, White PJ, Mills V, Pyke KA, Baker AJM, Whiting SN, May ST, Broadley MR. **2006**. A comparison of *Thlaspi caerulescens* and *Thlaspi arvense* shoot transcriptomes. *New Phytologist* **170**: 239–260.

Hanikenne M, Talke IN, Haydon MJ, Lanz C, Nolte A, Motte P, Kroymann J, Weigel D, Krämer U. **2008**. Evolution of metal hyperaccumulation required cis-regulatory changes and triplication of HMA4. *Nature* **453**: 391–395.

Hou X, Tong H, Selby J, DeWitt J, Peng X, He Z-H. **2005**. Involvement of a Cell Wall-Associated Kinase, WAKL4, in Arabidopsis Mineral Responses. *Plant Physiology* **139**:

1704–1716.

Jaffré T, Pillon Y, Thomine S, Merlot S. **2013**. The metal hyperaccumulators from New Caledonia can broaden our understanding of nickel accumulation in plants. *Frontiers in plant science* **4**: 279.

Jestrow B, Gutiérrez Amaro J, Francisco-Ortega J. **2012**. Islands within islands: A molecular phylogenetic study of the *Leucocroton alliance* (Euphorbiaceae) across the Caribbean Islands and within the serpentinite archipelago of Cuba. *Journal of Biogeography* **39**: 452–464.

Johnson MTJ, Carpenter EJ, Tian Z, Bruskiewich R, Burris JN, Carrigan CT, Chase MW, Clarke ND, Covshoff S, DePamphilis CW, *et al.* 2012. Evaluating Methods for Isolating Total RNA and Predicting the Success of Sequencing Phylogenetically Diverse Plant Transcriptomes. *PLoS ONE* **7**: e50226.

Karimi M, Inzé D, Depicker A. **2002**. GATEWAY™ vectors for *Agrobacterium*-mediated plant transformation. *Trends in Plant Science* **7**: 193–195.

Kasprzak MM, Erxleben A, Ochocki J. **2015**. Properties and applications of flavonoid metal complexes. *RSC Advances* **5**: 45853–45877.

Kopylova E, Noé L, Touzet H. **2012**. SortMeRNA: Fast and accurate filtering of ribosomal RNAs in metatranscriptomic data. *Bioinformatics* **28**: 3211–3217.

Krämer U. **2010**. Metal hyperaccumulation in plants. *Annual Review of Plant Biology* **61**: 517–534.

Krämer U, Cotter-Howells JD, Charnock JM, Baker AJM, Smith JAC. **1996**. Free histidine as a metal chelator in plants that accumulate nickel. *Nature* **379**: 635–638.

Krämer U, Pickering IJ, Prince RC, Raskin I, Salt DE. **2000**. Subcellular localization and speciation of nickel in hyperaccumulator and non-accumulator *Thlaspi* species. *Plant physiology* **122**: 1343–1353.

Krzesłowska M. **2011**. The cell wall in plant cell response to trace metals: polysaccharide remodeling and its role in defense strategy. *Acta Physiologiae Plantarum* **33**: 35–51.

Küpper H, Lombi E, Zhao FJ, Wieshammer G, McGrath SP. **2001**. Cellular compartmentation of nickel in the hyperaccumulators *Alyssum lesbiacum*, *Alyssum bertolonii* and *Thlaspi goesingense*. *J Exp Bot* **52**: 2291–2300.

Lanquar V, Ramos MS, Lelièvre F, Barbier-Brygoo H, Krieger-Liszkay A, Krämer U, Thomine S. **2010**. Export of Vacuolar Manganese by AtNRAMP3 and AtNRAMP4 Is Required for Optimal Photosynthesis and Growth under Manganese Deficiency. *Plant Physiology* **152**: 1986–1999.

Lešková A, Zvarík M, Araya T, Giehl RFH. **2019**. Nickel Toxicity Targets Cell Wall-Related Processes and PIN2-Mediated Auxin Transport to Inhibit Root Elongation and

734 Gravitropic Responses in Arabidopsis. *Plant and Cell Physiology* **0**: 1–17.
735 **Lin YF, Hassan Z, Talukdar S, Schat H, Aarts MG**. **2016**. Expression of the ZNT1 Zinc
736 Transporter from the Metal Hyperaccumulator *Noccaea caerulescens* Confers
737 Enhanced Zinc and Cadmium Tolerance and Accumulation to *Arabidopsis thaliana*.
738 *PLoS ONE* **11**: e0149750.
739 **Magallón S, Gómez-Acevedo S, Sánchez-Reyes LL, Hernández-Hernández T**. **2015**.
740 A metacalibrated time-tree documents the early rise of flowering plant phylogenetic
741 diversity. *New Phytologist* **207**: 437–453.
742 **Makarevitch I, Waters AJ, West PT, Stitzer M, Hirsch CN, Ross-Ibarra J, Springer**
743 **NM**. **2015**. Transposable Elements Contribute to Activation of Maize Genes in Response
744 to Abiotic Stress. *PLOS Genetics* **11**: 1–12.
745 **Matasci N, Hung L, Yan Z, Carpenter EJ, Wickett NJ, Mirarab S, Nguyen N, Warnow**
746 **T, Ayyampalayam S, Barker M, *et al.* 2014**. Data access for the 1 , 000 Plants (1KP)
747 project. *GigaScience* **3**: 1–17.
748 **Meier SK, Adams N, Wolf M, Balkwill K, Muasya AM, Gehring CA, Bishop JM, Ingle**
749 **RA**. **2018**. Comparative RNA-seq analysis of nickel hyperaccumulating and non-
750 accumulating populations of *Senecio coronatus* (Asteraceae). *The Plant Journal* **95**:
751 1023–1038.
752 **Merlot S, Hannibal L, Martins S, Martinelli L, Amir H, Lebrun M, Thomine S**. **2014**.
753 The metal transporter PgIREG1 from the hyperaccumulator *Psychotria gabriellae* is a
754 candidate gene for nickel tolerance and accumulation. *Journal of Experimental Botany*
755 **65**: 1551–1564.
756 **Mesjasz-Przybylowicz J, Przybylowicz W, Barnabas A, van der Ent A**. **2016**.
757 Extreme nickel hyperaccumulation in the vascular tracts of the tree *Phyllanthus balgooyi*
758 from Borneo. *New Phytologist* **209**: 1513–1526.
759 **Morrissey J, Baxter IR, Lee J, Li L, Lahner B, Grotz N, Kaplan J, Salt DE, Guerinot**
760 **ML**. **2009**. The ferroportin metal efflux proteins function in iron and cobalt homeostasis
761 in Arabidopsis. *Plant Cell* **21**: 3326–3338.
762 **Nishida S, Tsuzuki C, Kato A, Aisu A, Yoshida J, Mizuno T**. **2011**. AtIRT1, the primary
763 iron uptake transporter in the root, mediates excess nickel accumulation in *Arabidopsis*
764 *thaliana*. *Plant Cell Physiology* **52**: 1433–1442.
765 **Nishida S, Tanikawa R, Ishida S, Yoshida J, Mizuno T, Nakanishi H, Furuta N**. **2020**.
766 Elevated Expression of Vacuolar Nickel Transporter Gene IREG2 Is Associated With
767 Reduced Root-to-Shoot Nickel Translocation in *Noccaea japonica*. *Frontiers in Plant*
768 *Science* **11**: 610.
769 **Nkrumah PN, Baker AJM, Chaney RL, Erskine PD, Echevarria G, Morel JL, van der**
770 **Ent A**. **2016**. Current status and challenges in developing nickel phytomining: an

771 agronomic perspective. *Plant and Soil* **406**: 1–15.
772 **Oomen R, Wu J, Lelièvre F, Blanchet S, Richaud P, Barbier-brygoo H, Aarts MGM,**
773 **Thomine S**. **2008**. Functional characterization of NRAMP3 and NRAMP4 from the metal
774 hyperaccumulator *Thlaspi caerulescens*. *New Phytologist* **181**: 637–650.
775 **Pfaffl MW**. **2001**. A new mathematical model for relative quantification in real-time RT-
776 PCR. *Nucleic Acid Research* **29**: 16–21.
777 **Pillon Y, Hopkins HC, Rigault F, Jaffre T, Stacy EA**. **2014**. Cryptic adaptive radiation
778 in tropical forest trees in New Caledonia. *New Phytologist* **202**: 521–530.
779 **Pillon Y, Munzinger J, Amir H, Lebrun M**. **2010**. Ultramafic soils and species sorting
780 in the flora of New Caledonia. *Journal of Ecology* **98**: 1108–1116.
781 **R Development Core Team**. **2015**. R: A Language and Environment for Statistical
782 Computing. *R foundation for Statitical Computing*: http://www.R-project.org/.
783 **Reeves RD, Baker AJM, Jaffré T, Erskine PD, Echevarria G, van der Ent A**. **2018**. A
784 global database for plants that hyperaccumulate metal and metalloid trace elements.
785 *New Phytologist* **218**: 407–411.
786 **Ritchie ME, Phipson B, Wu D, Hu Y, Law CW, Shi W, Smyth GK**. **2015**. limma powers
787 differential expression analyses for RNA-sequencing and microarray studies. *Nucleic*
788 *Acid Research* **43**: e47.
789 **Robinson MD, McCarthy DJ, Smyth GK**. **2010**. edgeR: A Bioconductor package for
790 differential expression analysis of digital gene expression data. *Bioinformatics* **26**: 139–
791 140.
792 **Roux J, Rosikiewicz M, Robinson-Rechavi M**. **2015**. What to compare and how:
793 Comparative transcriptomics for Evo-Devo (M Robinson-Rechavi, Ed.). *Journal of*
794 *Experimental Zoology. Part B, Molecular and Developmental Evolution* **324**: 372–382.
795 **Schaaf G, Honsbein A, Meda AR, Kirchner S, Wipf D, von Wiren N**. **2006**. *AtIREG2*
796 encodes a tonoplast transport protein involved in iron-dependent nickel detoxification in
797 *Arabidopsis thaliana* roots. *Journal of Biological Chemistry* **281**: 25532–25540.
798 **Schwab R, Ossowski S, Riester M, Warthmann N, Weigel D**. **2006**. Highly Specific
799 Gene Silencing by Artificial MicroRNAs in *Arabidopsis*. *The Plant Cell* **18**: 1121–1133.
800 **Shahzad Z, Gosti F, Frérot H, Lacombe E, Roosens N, Saumitou-Laprade P,**
801 **Berthomieu P**. **2010**. The five *AhMTP1* zinc transporters undergo different evolutionary
802 fates towards adaptive evolution to zinc tolerance in *Arabidopsis halleri*. *PLoS Genetics*
803 **6**: e1000911.
804 **Simão FA, Waterhouse RM, Ioannidis P, Kriventseva E V, Zdobnov EM**. **2015**.
805 BUSCO: assessing genome assembly and annotation completeness with single-copy
806 orthologs. *Bioinformatics* **31**: 3210–3212.

Smith-Unna R, Boursnell C, Patro R, Hibberd J, Kelly S. **2016**. TransRate: reference free quality assessment of de novo transcriptome assemblies. *Genome Research* **26**: 1134–1144.

Tsai HH, Schmidt W. **2017**. Mobilization of Iron by Plant-Borne Coumarins. *Trends in Plant Science* **22**: 538–548.

Vacchina V, Mari S, Czernic P, Marques L, Pianelli K, Schaumloffel D, Lebrun M, Lobinski R. **2003**. Speciation of nickel in a hyperaccumulating plant by high-performance liquid chromatography-inductively coupled plasma mass spectrometry and electrospray MS/MS assisted by cloning using yeast complementation. *Analytical Chemistry* **75**: 2740–2745.

Verbruggen N, Hermans C, Schat H. **2009**. Molecular mechanisms of metal hyperaccumulation in plants. *New Phytologist* **181**: 759–776.

Waldron KJ, Rutherford JC, Ford D, Robinson NJ. **2009**. Metalloproteins and metal sensing. *Nature* **460**: 823–830.

Weber M, Harada E, Vess C, Roepenack-Lahaye E V, Clemens S. **2004**. Comparative microarray analysis of *Arabidopsis thaliana* and *Arabidopsis halleri* roots identifies nicotianamine synthase, a ZIP transporter and other genes as potential metal hyperaccumulation factors. *Plant Journal* **37**: 269–281.

Figure legends

Figure 1: Phylogenetic distribution of nickel hyperaccumulators. Eudicots Plant families containing nickel hyperaccumulators are indicated in red on the phylogenetic tree. The drawings illustrate the plant families and genera containing nickel hyperaccumulators that we have sampled from France, New Caledonia and Cuba.

Figure 2: Cross-family comparative transcriptomics and orthologous group annotation of genes convergently associated with nickel hyperaccumulation. (a) Cross-species comparative transcriptomic reveals Differential Expressed (DE) genes between nickel hyperaccumulator species (black) and related non-nickel accumulators (grey). Genes (contigs) are plotted according to their mean level of expression (x-axis) and their differential expression (y-axis) in the pair of species. The numbers of significant DE (red and blue dots) and non-DE genes are indicated ($log_2FC>1$, $FDR<0.05$). (b) Distribution of the 26 selected Cluster of Orthologous Groups (COGs) associated with nickel hyperaccumulation according to their predicted function and their level of expression in hyperaccumulators: COGs containing DE genes more expressed in nickel hyperaccumulators belonging to at least 3 distinct plant families (up-regulated COGs) are in red and COGs containing DE genes less expressed in nickel hyperaccumulators (down-regulated) are in blue. (c) Heat-maps of contigs associated with the selected COGs up-regulated in nickel hyperaccumulators from 5 distinct families. COGs corresponding to Class I transposable elements are not presented. (d) Heat-maps of contigs associated with down-regulated COGs. The color scale represents the expression Fold change of contigs in pairwise comparative analysis. The grey color represents the absence of contigs. Abbreviations: *Ncfi (Noccaea caerulescens subsp. firmiensis), Ncviv (N. caerulescens 'Viviez'), Nmon (N. montana), Pgra (Psychotria grandis), Prev (P. revoluta), Pcos (P. costivenia), Pgab (P. gabriellae), Psem (P. semperflorens), Gpru (Geissois pruinosa), Grac (G. racemosa)*, *Hkan (Homalium kanaliense)*, *Hbet (H. betulifolium), Lhav (Leucocroton havanensis)*, *Lmic (Lasiocroton microphyllus),* IREG/FPN (Iron Regulated/ Ferroportin), UGT85A (UDP-glucose:anthocyanidin/flavonol 3-O-glucosyltransferase), BAHD (BAHD acyltransferase), CYP71 (Cytochrome P450 71), CYP704 (Cytochrome P450 704), FAR (Fatty acyl-CoA reductase), SCPL (Serine carboxypeptidase), SSL (Strictosidine synthase), WAKL (Wall associated receptor kinase like), GLP (Germin-like protein), COR (Cold regulated gene), EXPA (Expansin), XTH (Xyloglucan endotransglucosylase/hydrolase), PAE (Pectin acetylesterase), CESA (Cellulose synthase), MLP (Major latex protein), JMT (Jasmonic acid carboxyl methyltransferase),

GDSL (GDSL esterase/lipase), GULLO (L-gulonolactone oxidase), LTP (Bifunctional inhibitor/lipid-transfer protein), DUF642 (DUF642 domain containing protein) and TPS (Terpene synthase).

Figure 3. Nickel sensitivity of yeast cells expressing plant IREG/Ferroportin transporters. Yeast cells expressing IREG/Ferroportin transporters cloned from *A. thaliana, N. caerulescens subsp. firmiensis, G. pruinosa and L. havanensis* were plated at different dilutions on a medium containing a toxic concentration of nickel for the control line (transformed with pDR195 vector).

Figure 4. Nickel accumulation and NcIREG2 expression in various accessions of Noccaea species. All plants were grown in hydroponic condition for 8 weeks in presence of 37.5 µM $NiCl_2$. (a) Nickel accumulation was measured in roots and shoots of *Noccaea caerulescens* 'Viviez' (*Ncviv*), *N. caerulescens subsp. firmiensis* (*Ncfi*) and *N. montana* (*Nmon*). Results are mean value ± SD (n = 3 biological replicates). Letters denote significant differences between accessions, with lowercase for roots and uppercase for shoots (Tukey HSD test, $p < 0.05$). (b) Quantitative RT-PCR analysis of NcIREG2 expression was performed on the same plants. *NcIREG2* expression was corrected using Nc6PGDH as a reference gene and normalized to 1 for the expression in *Ncviv*. Relative expression is displayed with a log2 scale. Results are mean value ± SD (n = 3 biological replicates).

Figure 5. Localization and silencing of the IREG/Ferroportin transporter NcfiIREG2 (a) NcfiIREG2 localizes on the vacuolar membrane in *N. caerulescens* cells. Confocal picture of a transgenic line expressing NcfiIREG2-GFP (green) in root cells. Cell wall was stained with propidium iodide (magenta). The scale bar corresponds to 5µm. (b) Silencing of the IREG/Ferroportin transporter *NcfiIREG2* in roots of the nickel hyperaccumulator *N. caerulescens subsp. firmiensis* reduces nickel accumulation. The expression of *NcfiIREG2* was quantified by RT-qPCR (black bars) in 8 amiRNA transgenic lines and control lines transformed with the pK7WG2D vector (n=3) growing in presence of 37.5 µM $NiCl_2$ for 4 weeks. *NcfiIREG2* expression was corrected using *Ncfi6PGDH* as reference gene and normalized to 1 for the expression in control lines. Nickel concentration was measured in parallel in roots of the same lines by MP-AES (green bars). (c) Correlation analysis between *NcfiIREG2* expression and nickel accumulation. The quadratic correlation model showed positive correlation (R^2 = 0.97**, *P-value* < 0.001) between *NcfiIREG2* expression and nickel accumulation in roots (black dots) and non-significant correlation (R^2 = 0.45) between *NcfiIREG2* expression in roots and nickel accumulation in shoots (grey dots).

Tables

Table 1. De novo assembled transcriptomes of nickel hyperaccumulators and related non-nickel accumulator species[$]

Family/Species	[Ni][#] (ppm)	Origin	Nbr. contigs	Assembly size (Mbp)	N50 (bp)
Brassicaceae - *Noccaea*					
Noccaea caerulescens subsp. firmiensis (Ncfi)	7580	France	41843	43.6	1735
N. caerulescens 'Viviez' *(Ncviv)*	239	France	na*	na*	na*
N. montana (Nmon)	916	France	87243	48.8	692
Rubiaceae - *Psychotria*					
Psychotria gabriellae (Pgab)	17618	New Caledonia	60899	45.5	1140
P. semperflorens (Psem)	34	New Caledonia	66755	49.8	1181
P. grandis (Pgra)	15176	Cuba	45143	36.8	1344
P. costivenia (Pcos)	1251[&]	Cuba	46451	35.1	1240
P. revoluta (Prev)	131	Cuba	56754	44.0	1245
Cunoniaceae - *Geissois*					
Geissois pruinosa (Gpru)	6239	New Caledonia	54969	42.1	1243
G. racemosa (Grac)	132	New Caledonia	58386	43.7	1021
Salicaceae - *Homalium*					
Homalium kanaliense (Hkan)	6342	New Caledonia	52634	40.6	1259
H. betulifolium (Hbet)	275	New Caledonia	49962	39.0	1294
Euphorbiaceae – Adelieae tribe					
Leucocroton havanensis (Lhav)	14073	Cuba	58990	44.4	1206
Lasiocroton microphyllus (Lmic)	43	Cuba	52421	39.8	1244

[$] Details are provided in Supporting Information Table S1 and S2
[#] Mean nickel concentration measured in leaves (n=2, Table S1)
* not assembled: The transcriptome of *Ncfi is used as a reference for Ncviv*
[&] Concentration likely underestimated because the samples were conserved in water-based RNA*later*

905 **The following Supporting Information is available for this article:**

906 **Figure S1:** Estimated time-divergence between species used in this study

907 **Figure S2:** Workflow used for RNA-Seq analyses

908 **Figure S3:** Additional MA-plot representation of cross-species comparative
909 transcriptomic analyses

910 **Figure S4:** Effect of the choice of the reference transcriptome on the identification of
911 Differentially Expressed genes

912 **Figure S5:** Molecular phylogeny of the plant IREG/Ferroportin family

913 **Figure S6:** Expression of *IREG/Ferroportin* orthologs in *Homalium* and *Geissois* species

914 **Figure S7:** The NcfiIREG2-GFP fusion protein is functional in *A. thaliana*

915 **Table S1:** Metadata associated with plant samples

916 **Table S2:** RNA-Seq sequencing, assembly and mapping statistics

917 **Table S3:** Cluster of Orthologous Group analysis metrics

918 **Table S4:** Differentially Expressed Genes analysis

919 **Table S5:** List of Cluster of Orthologous Group associated with nickel hyperaccumulation

920 **Table S6:** List of primers.

921 **Notes S1:** References for Supporting Information
922

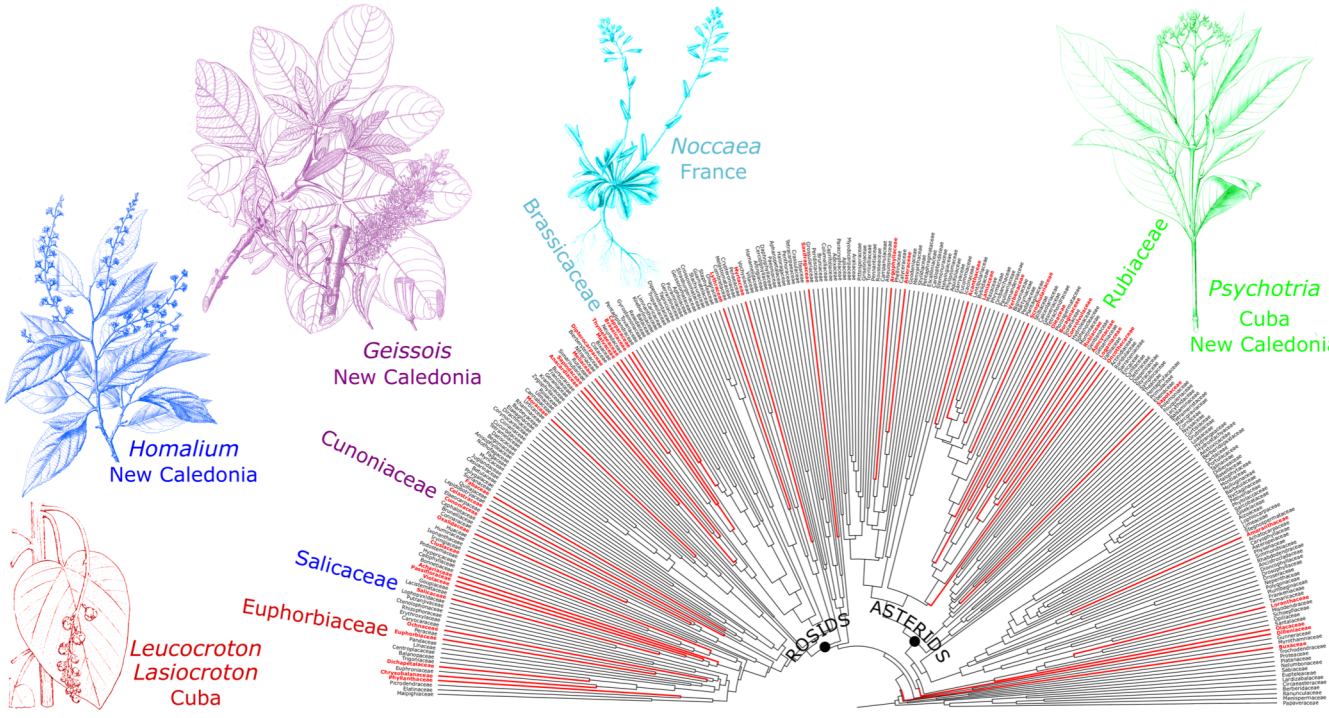
Noccaea
France
Brassicaceae
Rubiaceae
Psychotria
Cuba
New Caledonia
Geissois
New Caledonia
Homalium
New Caledonia
Cunoniaceae
Salicaceae
Euphorbiaceae
Leucocroton
Lasiocroton
Cuba
ROSIDS
ASTERIDS

Figure 1

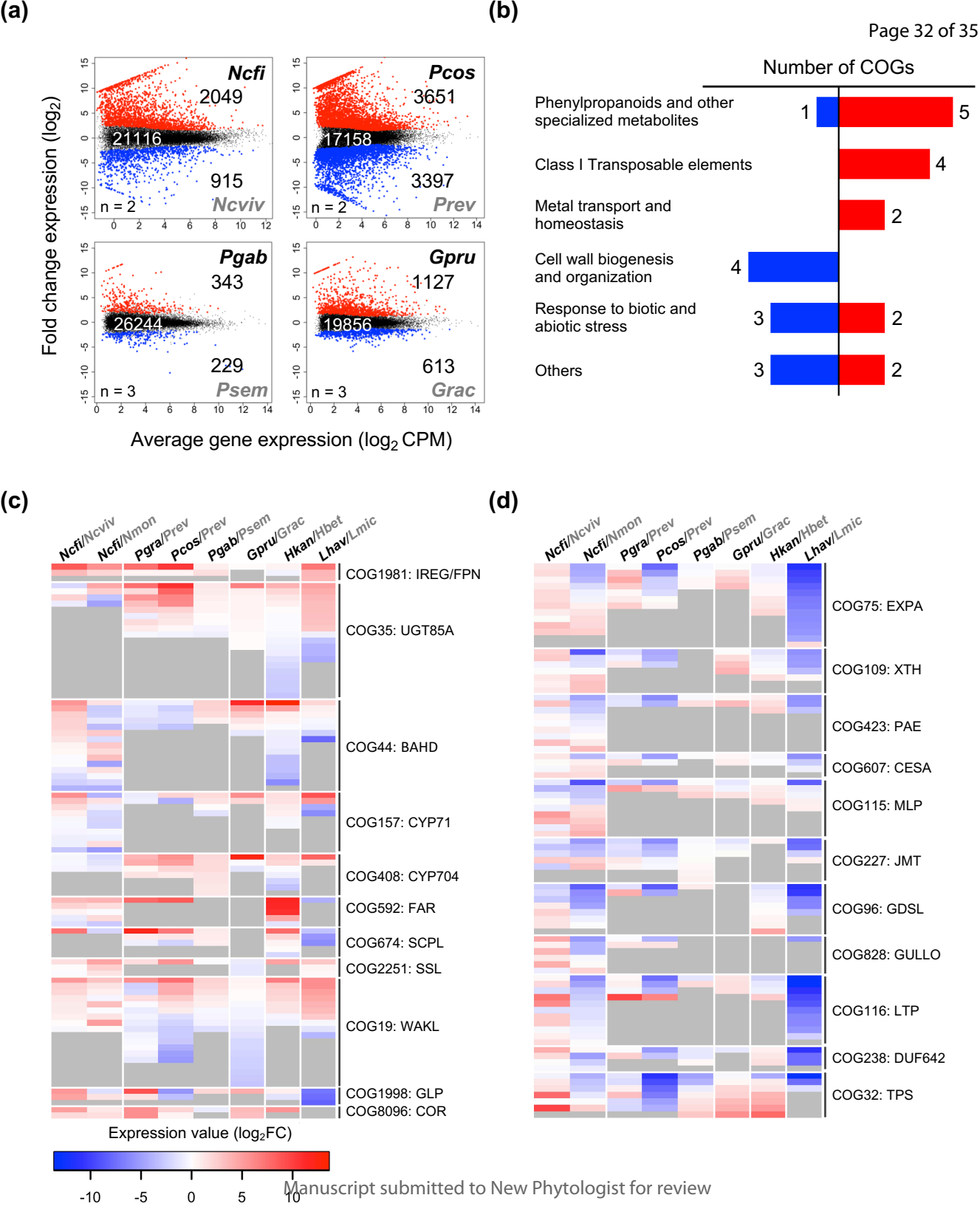
(a)
Ncfi
2049
21116
915
n = 2
Ncviv
Pcos
3651
17158
3397
n = 2
Prev
Pgab
343
26244
229
n = 3
Psem
Gpru
1127
19856
613
n = 3
Grac
Fold change expression (log2)
Average gene expression (log2 CPM)
(b)
Number of COGs
Phenylpropanoids and other specialized metabolites
1
5
Class I Transposable elements
4
Metal transport and homeostasis
2
Cell wall biogenesis and organization
4
Response to biotic and abiotic stress
3
2
Others
3
2
(c)
Ncfi/Ncviv
Ncfi/Nmon
Pgra/Prev
Pcos/Prev
Pgab/Psem
Gpru/Grac
Hkan/Hbet
Lhav/Lmic
COG1981: IREG/FPN
COG35: UGT85A
COG44: BAHD
COG157: CYP71
COG408: CYP704
COG592: FAR
COG674: SCPL
COG2251: SSL
COG19: WAKL
COG1998: GLP
COG8096: COR
Expression value (log2FC)
-10
-5
0
5
10
(d)
COG75: EXPA
COG109: XTH
COG423: PAE
COG607: CESA
COG115: MLP
COG227: JMT
COG96: GDSL
COG828: GULLO
COG116: LTP
COG238: DUF642
COG32: TPS

Figure 2

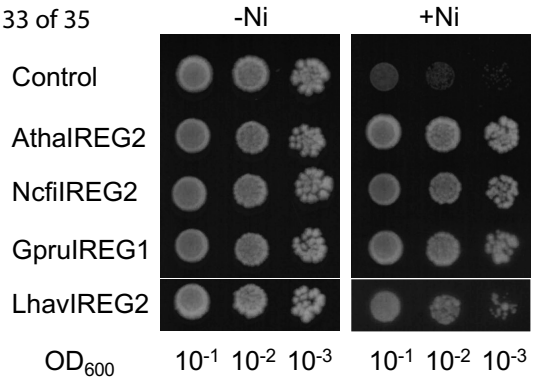
-Ni
+Ni
Control
AthaIREG2
NcfiIREG2
GpruIREG1
LhavIREG2
OD600
10-1 10-2 10-3
10-1 10-2 10-3

Figure 3

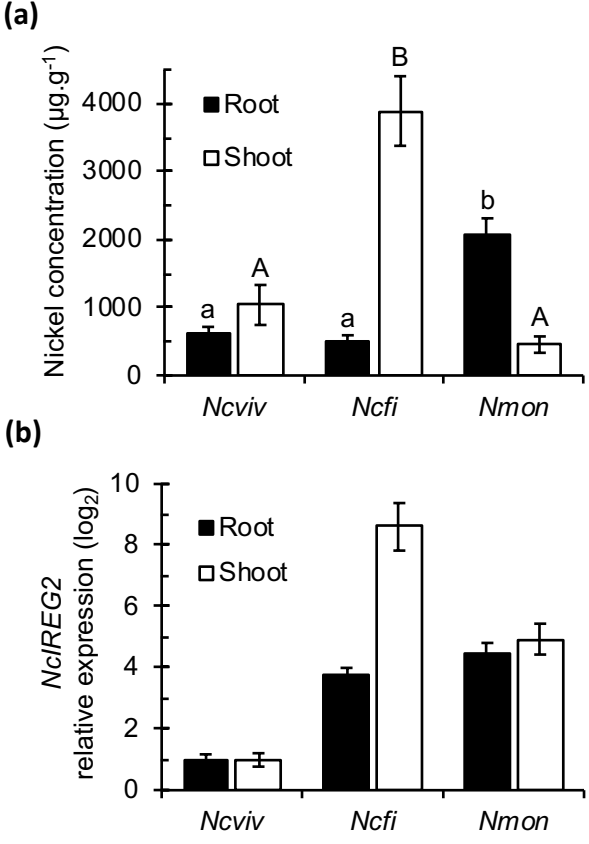
(a)
Nickel concentration (µg.g-1)
4000
3000
2000
1000
0
Root
Shoot
a
A
a
B
b
A
Ncviv
Ncfi
Nmon
(b)
NclREG2
relative expression (log2)
10
8
6
4
2
0
Root
Shoot
Ncviv
Ncfi
Nmon

Figure 4

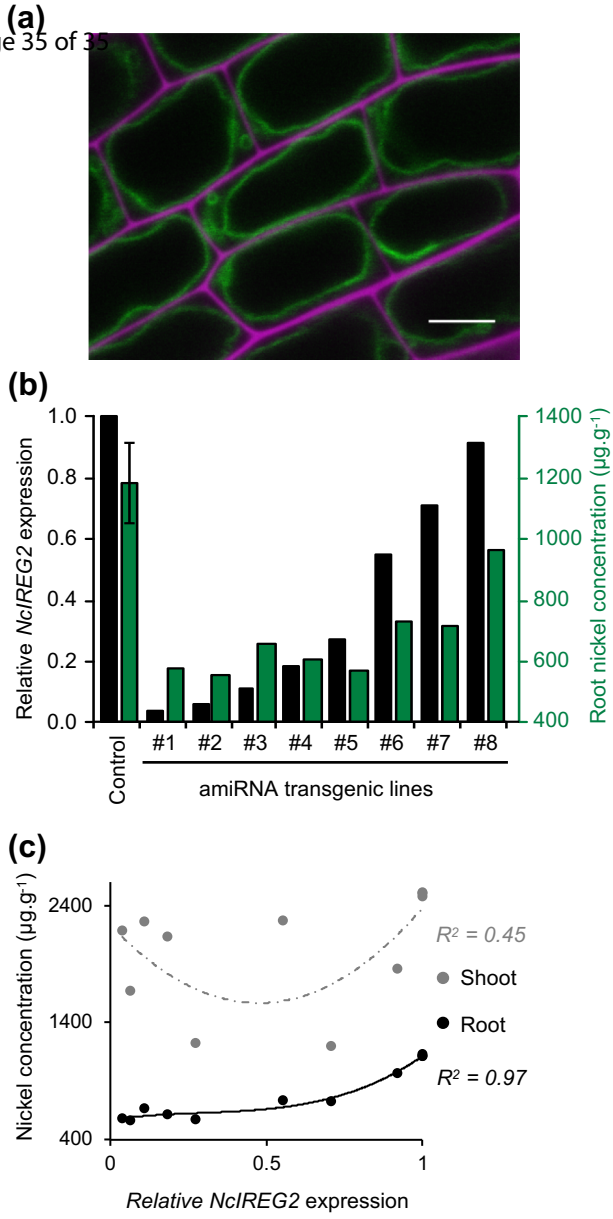
(a)
(b)
Relative NcIREG2 expression
Root nickel concentration (µg.g-1)
1.0
0.8
0.6
0.4
0.2
0.0
1400
1200
1000
800
600
400
Control
#1
#2
#3
#4
#5
#6
#7
#8
amiRNA transgenic lines
(c)
Nickel concentration (µg.g-1)
2400
1400
400
0
0.5
1
Relative NcIREG2 expression
R² = 0.45
Shoot
Root
R² = 0.97

Figure 5